First Ply Failure Analysis of Rectangular Fiber Metal Laminated Composite Plates Subjected to Uniformly Distributed Loads

Nandure Narayan Rao & Pavuluri M. V. Rao

Journal of Failure Analysis and Prevention

ISSN 1547-7029

J Fail. Anal. and Preven.
DOI 10.1007/s11668-019-00768-x

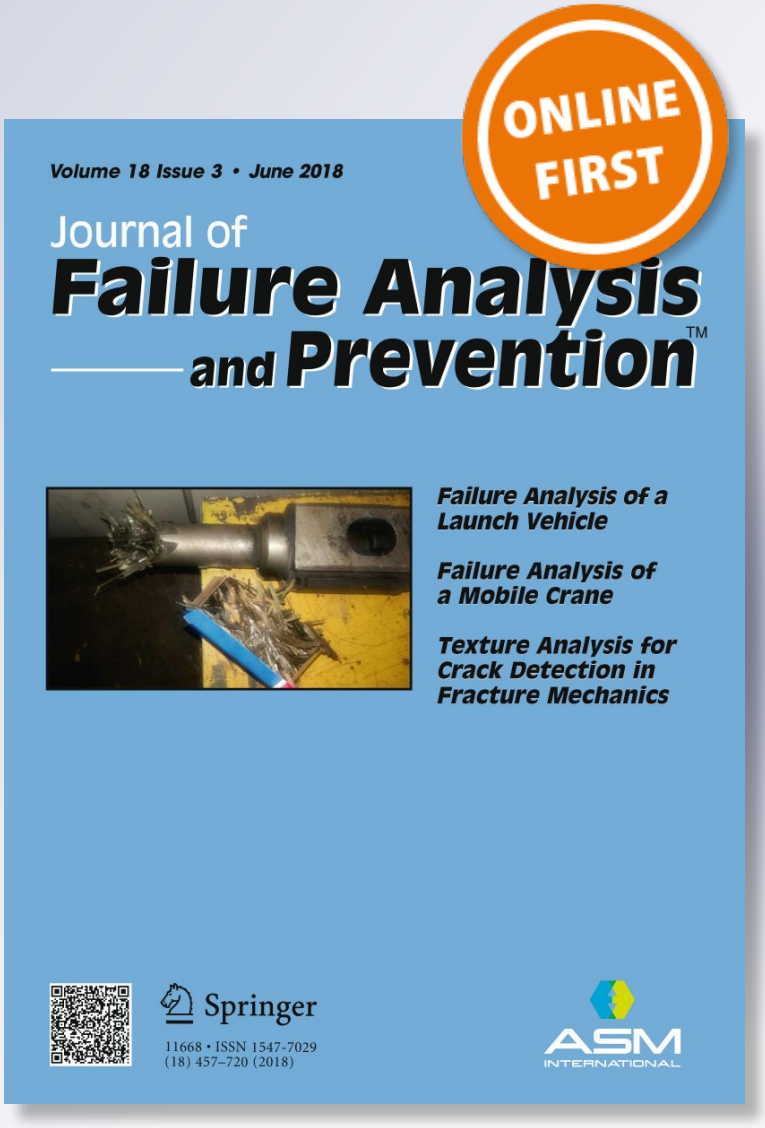

Springer

J Fail. Anal. and Preven.
https://doi.org/10.1007/s11668-019-00768-x

TECHNICAL ARTICLE—PEER-REVIEWED

First Ply Failure Analysis of Rectangular Fiber Metal Laminated Composite Plates Subjected to Uniformly Distributed Loads

Nandure Narayan Rao · Pavuluri M. V. Rao

Submitted: 7 April 2019

Abstract Fiber metal laminates (FMLs) are the hybrid composite materials that needed analysis for using them toward applications as rectangular plates subjected to uniformly distributed loads. Determination of first ply failure (FPF) loads is the focus of the present study. These loads are identified by the procedure developed on the basis classical laminate theory (CLT), and Tsai–Hill criterion is used to identify the failure load. The developed procedure was validated by applying it to the standard cases reported in the literature. The failure loads and deformation of FMLs are presented in the form of dimensionless parameters, and their variation was studied for width-to-length ratios. FMLs of GLARE and Ti-CFRP are studied based on their importance to research.

Keywords First ply failure · Fiber metal laminates · Uniformly distributed load · Classical laminate theory

Introduction

Fiber metal laminates (FML) are the hybrid composite laminates consisting of metal layers and fiber reinforced polymer layers as laminas. These materials are introduced in 1978 at Delft University of Technology [1], and initial configurations consist of thin high strength aluminum alloy sheets alternately bonded to the plies of glass fiber reinforced epoxy laminas. These materials can be designed to have a specific improvement in properties [2] like fatigue resistance, impact resistance, corrosion resistance, etc. Promising applications of this type of material encouraged the researchers to do experimentation with various types of metal layers and FRP layer layup orientations. FMLs with GFRP layers and aluminum metal layers are grouped under a family called as GLARE [3, 4] and are extensively investigated. This leads to the application of GLARE as fuselage structural material for Airbus A380 [5]. One more material group under the family of FML is the ARALL [5], with aramid fiber/epoxy prepreg and aluminum layers. Many new materials are also under investigation such as CFRPs with titanium layers [6, 7] CFRPs with magnesium layers [8, 9].

Satisfactory analytical techniques to predict the behavior and the availability of the data related to the behavior aspects of the material are the requirements to consider material for an engineering application. For this purpose, various researchers have published useful data for FMLs. Fatigue, fracture and impact response of various grades of GLARE are investigated [3] and reported. Analytical techniques to predict the behavior of stress–strain, impact, delamination are reported by investigators [10–15] as a support to the experimental analysis. Literature review reveals that similar type of exercises is being carried out for other type of FMLs also [6, 8, 9, 16]. It can be observed that much of the research information available in public domain is about the behavior of FML under in-plane loads, fatigue loads and impact loads. Very less information is available on the behavior of FML as a plate subjected to loads on a surface such as uniformly distributed pressure. Probably because the former type of loadings is more dominant, FMLs are expected to be used. However, the knowledge about this aspect is very much essential to extend the use of FMLs to other applications: as happened

N. Narayan Rao (✉) · P. M. V. Rao
Vignan's Foundation for Science Technology and Research, Guntur, India
e-mail: nandurerao@gmail.com

Published online: 17 October 2019

in general composite materials. The work presented here is an attempt in this regard.

A brief literature survey is presented here to identify the existing procedures for the analysis of composite plates subjected to uniformly distributed loads. Initial results from the flexural analysis of symmetrically laminated cross-ply rectangular plates are made by combining Navier's solutions with Tsai–Hill failure criterion [17]. The study is restricted to symmetric cross-ply layups that exhibit flexurally orthotropic properties. The FPFs are estimated for various aspect ratios. A finite element-based procedure combined with classical laminate theory (CLT) is used to predict the FPF loads of various types of composite laminate configurations [18], and good correlation was reported between predictions and exact solutions. Over the period of time, similar approaches with different types of elements and configurations are reported along with the various analysis techniques [19, 20]. New techniques such as hybrid semi-analytical methods continue to emerge for the bending analysis of multilayered composite plates [21]. From the literature survey, it is established that CLT forms the basis for the majority of analytical techniques due to its simplicity. It can be also observed that the plate behavior is explained with the help of parameters like FPFs, deflections and the variation of these parameters with the plate aspect ratios. Based on this background, the major steps in the present analysis are identified as (a) developing a procedure based on CLT to calculate stresses and deflections, (b) validation of the procedure, (c) using the procedure for the FML and (d) analysis of results.

Selecting an appropriate failure theory is a major step in this type of procedures, and the Tsai–Hill theory is the simplest, interactive and reasonably accurate theory out of various theories available for this purpose [21]. In view of this, Tsai–Hill theory is incorporated in present analysis to identify the failure of the lamina. The analysis is also restricted to uniaxial and cross-ply laminates, since the majority of the FMLs reported are of similar construction.

Formulation

The formulations of the classical laminate theory (CLT) are widely published, and only major steps in the CLT that are relevant to the present procedure are mentioned here [22]. According to this theory, the forces (N) and moments (M) acting on the laminate are related to in-plane strains (ε^0) and curvatures (k) by

$$\begin{bmatrix} N \\ M \end{bmatrix} = \begin{bmatrix} A & B \\ B & D \end{bmatrix} \begin{bmatrix} \varepsilon^0 \\ \kappa \end{bmatrix} \quad \text{(Eq 1)}$$

A, B and D are 3×3 matrices linking the forces and moments to the strains and curvatures. For the present problem of symmetric laminate configuration, for cross-ply or uniaxial, it can be shown that $A_{16} = A_{26} = D_{16} = D_{26} = 0$; and $B_{ij} = 0$ for all i and j.

Solving Eq 1 for a simply supported rectangular laminate with a uniformly distributed load on its surface the following expressions can be obtained for the strains at any point x, y and z within the laminate. The configuration of the plate is shown in Fig. 1 [23]

$$\varepsilon_x = z \sum_{m=1,3}^{\infty} \sum_{n=1,3}^{\infty} W_{mn} \left(\frac{m\pi}{a}\right)^2 \cos\left(\frac{m\pi x}{a}\right) \cos\left(\frac{n\pi y}{b}\right)$$

$$\varepsilon_y = z \sum_{m=1,3}^{\infty} \sum_{n=1,3}^{\infty} W_{mn} \left(\frac{n\pi}{b}\right)^2 \cos\left(\frac{m\pi x}{a}\right) \cos\left(\frac{n\pi y}{b}\right)$$

$$\gamma_{xy} = -2z \sum_{m=1,3}^{\infty} \sum_{n=1,3}^{\infty} W_{mn} \left(\frac{n\pi}{b}\right) \left(\frac{m\pi}{a}\right) \sin\left(\frac{m\pi x}{a}\right) \sin\left(\frac{n\pi y}{b}\right) \quad \text{(Eq 2)}$$

The deflections can be calculated from

$$\omega^0(x, y) = \sum_{m=1,3}^{\infty} \sum_{n=1,3}^{\infty} W_{mn} \left(\frac{m\pi}{a}\right)^2 \cos\left(\frac{m\pi x}{a}\right) \cos\left(\frac{n\pi y}{b}\right) \quad \text{(Eq 3)}$$

Appropriate stress–strain relations are used for arriving at stress values. The entire procedure of calculation of stresses and deflections is computerized by using MATLAB routine. Figures 2 and 3 shows the program output for two configurations of the graphite–polymer composite; for validation, these results are compared with the results available in publications [22], and good correlation is observed.

With the continuous increase of load on the surface, the stresses in laminas will also increase and a stage will be

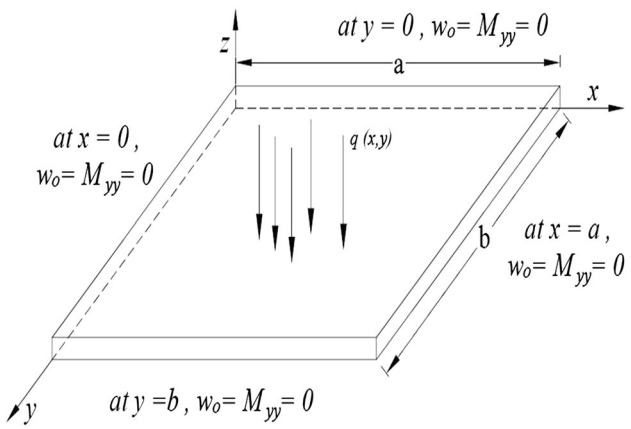

Fig. 1 Simply supported rectangular plate subjected uniformly distributed load

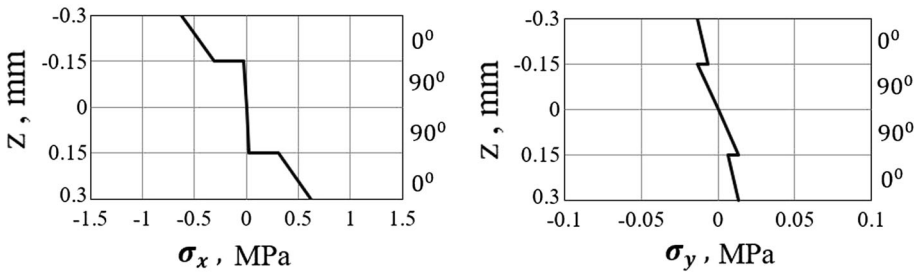

Fig. 2 Stresses at the center of pressure loaded, simply supported, rectangular $[0/90]_s$ plate (b/a = 2)

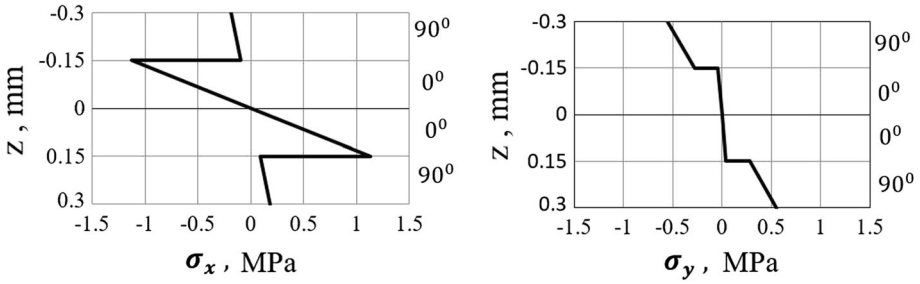

Fig. 3 Stresses at the center of pressure loaded, simply supported, rectangular $[90/0]_s$ plate (b/a = 2)

reached where the stress state in a particular lamina will satisfy the selected failure criterion. According to the Tsai–Hill criterion, the failure of a lamina will occur when the stresses satisfy the following equation [14].

$$\frac{\sigma_1^2}{X^2}+\frac{\sigma_2^2}{Y^2}+\frac{\tau_{12}^2}{S^2}-\frac{\sigma_1\sigma_2}{X^2}\geq 1 \qquad \text{(Eq 4)}$$

where σ_1, σ_2 and τ_{12} are the principal stresses and shear stress in the lamina, respectively. X, Y and S are the longitudinal tensile/compressive strength, transverse tensile/compressive strength and shear strength, respectively. The selection between tensile and compressive strengths will be made from the nature of principle stresses.

To validate the developed program for FPF estimation, for simply supported rectangular plates having width-to-length ratio (b/a), different orientations of plies have been considered. The plate loading along with boundary conditions is described in Fig. 1, the strength and material properties are given in Table 1 two-dimensional less parameters presented in the literature, i.e., $\bar{q}$ (FPF load) and $\bar{w}$ (transverse central deflection) are used as behavioral parameters [19] and they are $\bar{q}=q_0a^2h^{-2}S_{2T}^{-1}$ and $\bar{w}=w_0D_Ta^{-2}S_{2T}^{-1}h^{-2}$, (where $D_T=E_2h^3/(1-v_{12}v_{21})12$ is plate flexural rigidity), respectively. The first case taken up for validation is a cross-ply laminate with 0/90 configuration [17]. The variation of FPF load for different layup of GFRP is shown in Fig. 4.

From Fig. 4, it can be observed that the influence of laminate thickness on FPF load is more for smaller aspect ratios, whereas for larger aspect ratios, the gain in FPF strengths is small between the three laminates. The variation in FPF load with the aspect ratio is considerable up to ratio 2, and beyond this, the FPF load remained constant

Table 1 Material strength properties

Properties	Ti–Metal [6]	2024 T3 Al [24]	S2/FM94 GFRP [16]	CFRP [6]
Longitudinal modulus E_1 (Gpa)	100	71.1	48.6	125
Transverse modulus E_2 (Gpa)	100	71.1	8.5	8.9
Shear modulus G_{12} (Gpa)	43	27.2	3.1	5
Poisson ratio ν_{12}	0.33	0.33	0.33	0.33
Tensile strength in fiber direction X_T (Mpa)	1210	455	1900	1693
Tensile strength transverse to fiber direction Y_T (Mpa)	1210	455	56	78
In-plane shear strength S_{12} (Mpa)	295	248	38	157
Thickness of single lamina (mm)	0.14	0.205	0.26	0.135

for all the three configurations. The FPF loads and deflections in dimensionless form are presented in Figs. 5 and 6. All the results have been found to be in good agreement with the exact solutions reported in literature [17], thus validating the procedure for identifying the FPF loads.

FPF Analysis of FMLs

After ensuring the accuracy of the present procedure in the calculation of FPF loads and deflections, the procedure is used to predict the FPF loads of FMLs of different configurations. The materials and configurations are selected

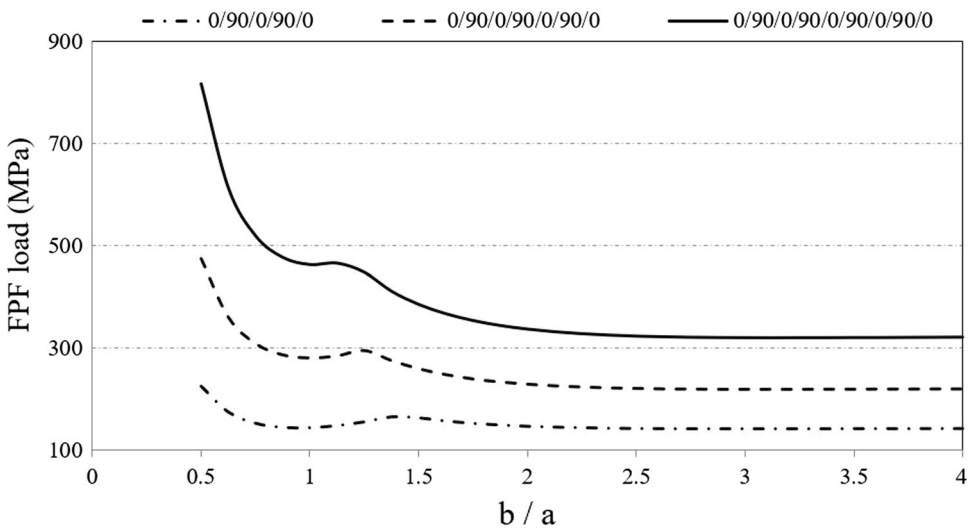

Fig. 4 Variation of FPF load with plate aspect ratio (b/a)

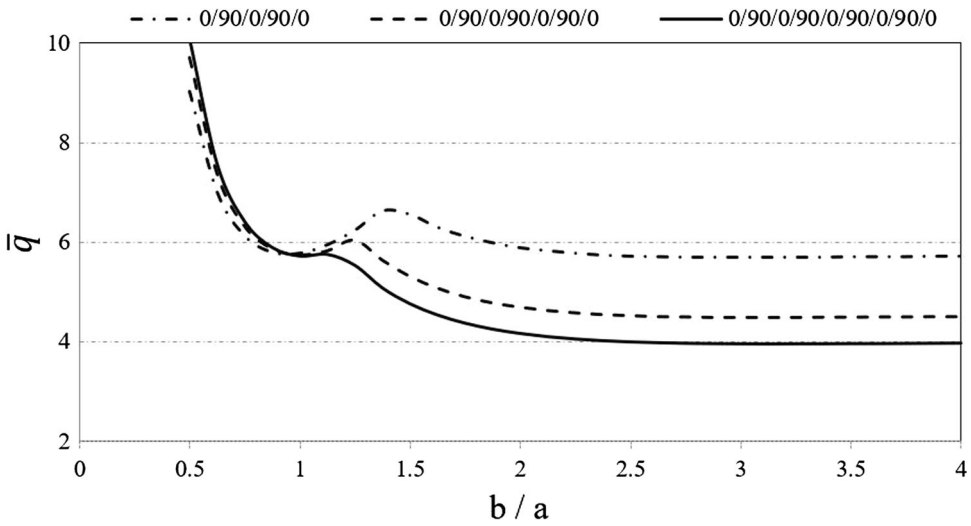

Fig. 5 Variation of non-dimensional FPF parameter $\bar{q}$ with plate aspect ratio (b/a)

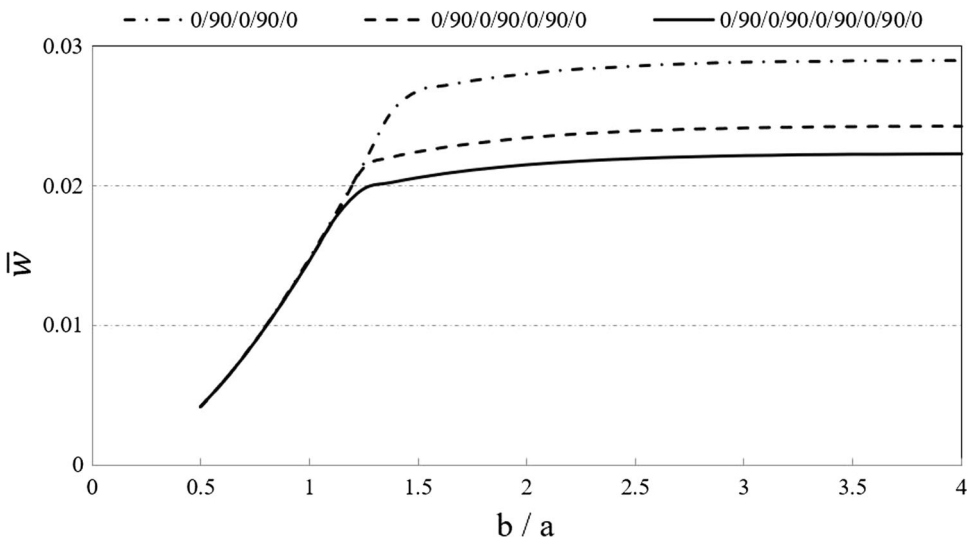

Fig. 6 Variation of non-dimensional deflection parameter $\bar{w}$(at FPF) with plate aspect ratio (b/a)

from the recently reported literature so that only the cases related to the on-going research are taken up for study. These materials are (1) Ti-CFRP, configuration [Ti/0/0/0/0/Ti], (2) Al-GFRP, configuration [Al/0/90/Al/90/0/Al]. Some more configurations derived from these materials are added to the analysis for the purpose of academic interest.

Nature of Failure

Identifying the nature of failure is an essential part in the stress–strain analysis. Many approximations are reported in the literature; one of the techniques proposed is based on the values of terms in the Tsai–Hill criterion when the failure condition is satisfied [25]. At the time of failure, if the first ratio in the Tsai–Hill equation "σ_1^2/X^2" value is more compared to other ratios, then it can be approximated as failure along the fiber direction and designated as "Mode I" failure. Similarly, if "σ_2^2/Y^2" value is larger, then the failure can be called as failure in transverse to fiber direction and designated as "Mode II" failure. The tensile and compressive failure can be predicted from the sign of the stress values at the time of failure.

Titanium-Carbon Fiber/PEEK Laminate [26]

Three configurations from this material group are analyzed for the FPF behavior. Failure of the composite layers is taken as the criterion to identify the FPF of the laminate. The results are shown in Figs. 7 and 8. From the Figs, it can be observed that the behavior of [Ti/0/0/0/0/Ti] laminate is similar to [Ti/0/90/90/0/Ti] laminate. The nature of the failures predicted is also the same for both the laminates. The failure surface is the bottom of last CFRP layer and in mode II for aspect ratios less than 1.375. For aspect ratios larger than this, the failure is observed at the top of the first CFRP layer and in mode I. The larger span increases the deflection, and thus, increasing the stress in the top and bottom layers leads to the mode I failure. This transition in the mode of failure is highlighted by nick on the diagram, as shown in Fig. 7.

The laminate [Ti/90/0/0/90/Ti] has shown a different trend. The nature of the failures is also different with the mode I failures for aspect ratios up to 0.875, and beyond this, the failures are of mode II. Mode I failures are observed at the upper surface of the topmost CFRP layer, and mode II type failures are reported at the lower surface of the bottom CFRP layer. The reason behind this behavior is for aspect ratios at 0.875; the longer span is along the fiber orientation of top and bottom CFRP layers. For aspect ratios greater than this, the stresses in the transverse to fiber direction of top and bottom layers will be large and failure has occurred in mode II. As shown in Fig. 8, the deflections remain more or less the same for all the three cases.

Aluminum-GFRP Laminate with a Central Metal Layer [27]

Three configurations from this material group are analyzed for the FPF behavior. Failure of the composite layers is taken as the criterion to identify the FPF of the laminate. Figure 9 shows the variation of $\bar{q}$ with aspect ratio.

It can be observed that for the configurations [Al/0/0/Al/0/0/Al] and [Al/0/90/Al/90/0/Al], the FPF strength is the same for aspect ratio up to 1.375. After this aspect ratio, the difference in strength is gradually increased with higher

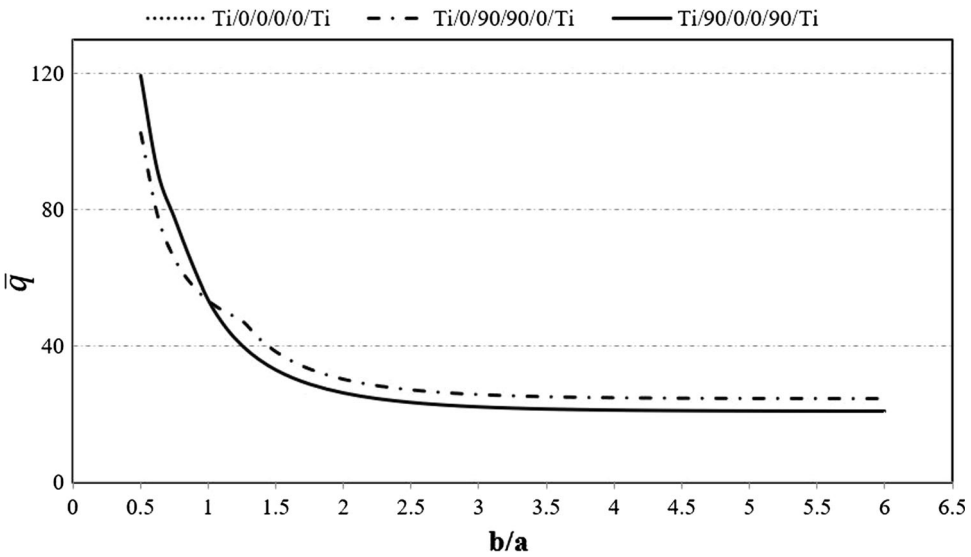

Fig. 7 Variation of non-dimensional FPF parameter $\bar{q}$ with plate aspect ratio (b/a)

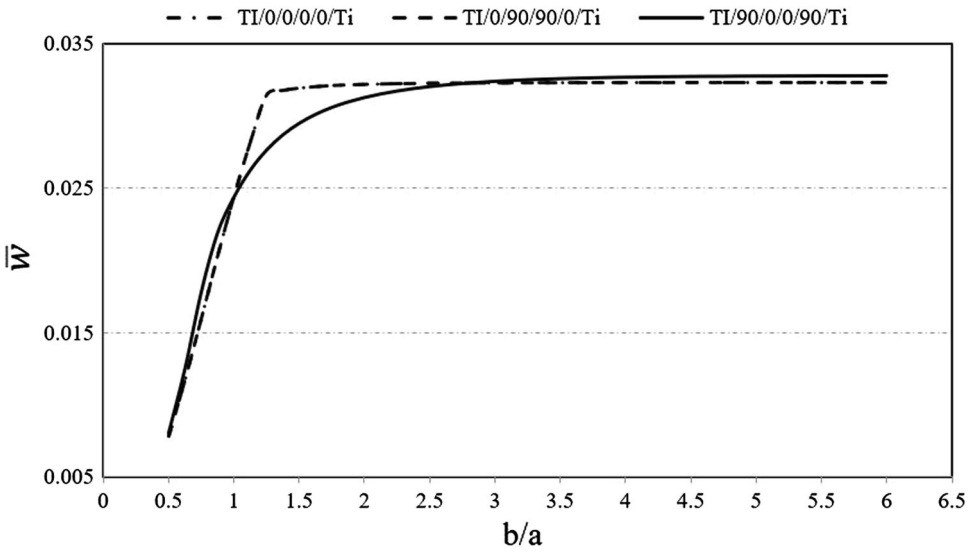

Fig. 8 Variation of non-dimensional deflection parameter $\bar{w}$ (at FPF) with plate aspect ratio (b/a)

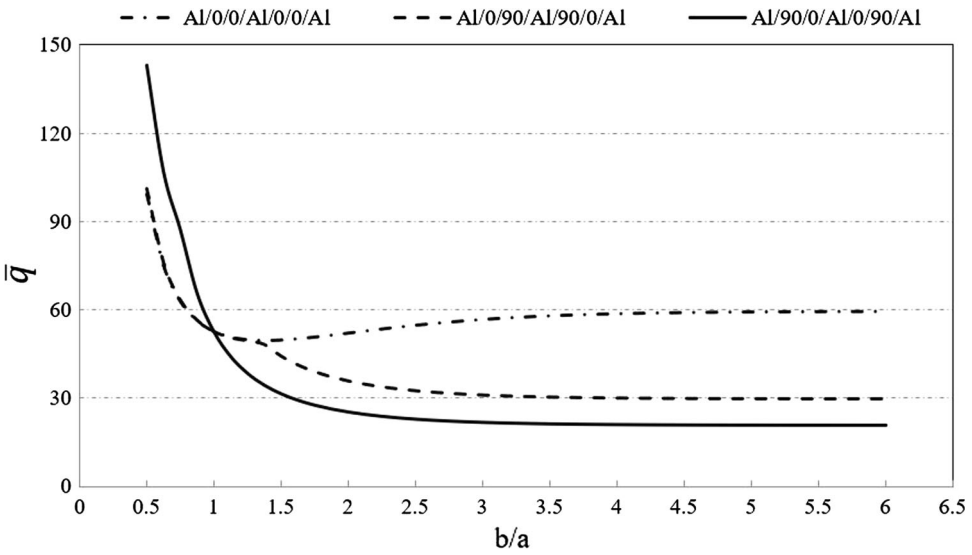

Fig. 9 Variation of non-dimensional FPF parameter $\bar{q}$ for three configurations

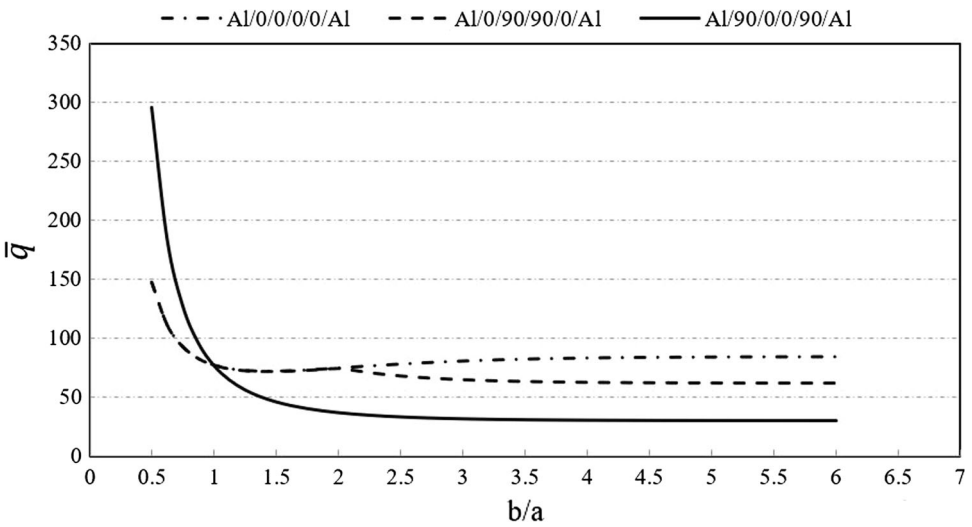

Fig. 10 Variation of non-dimensional FPF parameter $\bar{q}$ for three configurations without a central metal layer

strength [Al/0/0/Al/0/0/Al]. The results also show that for aspect ratios smaller than one, higher strengths can be achieved by placing the (90°) layer on top.

The failure in [Al/0/0/Al/0/0/Al] laminate for all aspect ratios is in mode II and can be taken as matrix dominated. For [Al/0/90/Al/90/0/Al] laminate, the failures have occurred on the top surface of the first GFRP layer (0°) in mode II for aspect ratios up to 1.25. Later, the failure has occurred on the top surface of the second GFRP layer (90°) in mode II. For [Al/90/0/Al/0/90/Al], the failures have occurred on the top surface of the second GFRP layer (0°) in mode II for aspect ratios up to 0.625. Later, the failure has occurred on the top surface of the first GFRP layer (90°) in mode II.

Aluminum-GFRP Laminate (Without a Central Metal Layer) [28]

Three configurations from this material group without a central metal layer are analyzed for the FPF behavior. The results of FPF variation for laminate with the aspect ratio are shown in Fig. 10. It can be observed that the $\bar{q}$ variation of [Al/0/0/0/0/Al] is same with [Al/0/90/90/0/Al] up to aspect ratio 2.125, after this difference in strength can be observed with higher strength for [Al/0/0/0/0/Al]. For aspect ratio less than 1, [Al/0/90/90/0/Al] has shown higher strength compared to other two laminates.

The failure of [Al/0/0/0/0/Al] is in mode II for all aspect ratios and on top of GFRP, whereas for [Al/0/90/90/0/Al] for small aspect ratio, failure happened on top GFRP layer in mode II and for aspect ratio greater than 2 it happened on 90° layer and in mode II. The failure of [Al/90/0/0/90/Al] has happened in mode II and on top GFRP layer. When compared with the strength of FML with a metal layer as a central layer, all the three laminates without central metal layer have shown higher strength. This behavior can be attributed to the increase of distance from the neutral layer to the top/bottom layers, which increases the bending stress, thus leading to the failure at smaller loads.

Conclusion

It was established that the FMLs are the promising materials for industrial applications and there is a requirement to analyze their behavior as plate subjected to uniformly distributed loads. An analytical approach to predict the first ply failure loads was developed and validated. By using the approach, FPF loads for three FML configurations are estimated and the variation of FPF loads with plate aspect ratios presented. The results showed that.

(a) After an aspect ratio, the FPFs loads remain constant and depend upon configurations.
(b) For small aspect ratios of less than 1, higher strengths are possible by placing top and bottom composite layers, parallel to the shorter side.
(c) While designing FMLs for applications as plate subjected to UDL, incorporation of central metal layers may not have a positive effect on the strength.

References

1. A. Asundi, A.Y.N. Choi, Materials processing technology fiber metal laminates: an advanced material for future aircraft. J. Mater. Process. Technol. **63**(1–3), 384–394 (1997)
2. L.B. Vogelesang, A. Vlot, Development of fibre metal laminates for advanced aerospace structures. J. Mater. Process. Technol. **103**(1), 1–5 (2000)
3. G.H.J.J. Roebroeks, Fibre-metal laminates: recent developments and applications. Int. J. Fatigue **16**(1), 33–42 (1994)
4. E. Cocchieri, R. Almeida, S. José, S. Paulo, A review on the development and properties of continuous fiber/epoxy/aluminum hybrid composites for aircraft structures. Mater. Res. **9**(3), 247–256 (2006)
5. T. Sinmazçelik, E. Avcu, M.Ö. Bora, O. Çoban, A review: fibre metal laminates, background, bonding types and applied test methods. Mater. Des. **32**(7), 3671–3685 (2011)
6. P. Cortes, W.J. Cantwell, The tensile and fatigue properties of carbon fiber-reinforced PEEK-titanium fiber-metal laminates. J. Reinf. Plast. Compos. **23**(15), 1615–1623 (2004)
7. W. Steve, J. Edward, High temperature hybrid titanium composite laminates: an early analytical assessment. Appl. Compos. Mater. **3**, 379–390 (1996)
8. P. Cortés, W.J. Cantwell, Fracture properties of a fiber-metal laminates based. J. Mater. Sci. **39**(3), 1081–1083 (2004)
9. R. Alderliesten, C. Rans, R. Benedictus, The applicability of magnesium based fibre metal laminates in aerospace structures. Compos. Sci. Technol. **68**(14), 2983–2993 (2008)
10. S.U. Khan, R.C. Alderliesten, R. Benedictus, Delamination in fiber metal laminates (GLARE) during fatigue crack growth under variable amplitude loading. Int. J. Fatigue **33**(9), 1292–1303 (2011)
11. Y. Huang, J. Liu, X. Huang, J. Zhang, G. Yue, Delamination and fatigue crack growth behavior in fiber metal laminates (Glare) under single overloads. Int. J. Fatigue **78**(September), 53–60 (2015)
12. J. Chen, E.V. Morozov, K. Shankar, Progressive failure analysis of perforated aluminium/CFRP fibre metal laminates using a combined elastoplastic damage model and including delamination effects. Compos. Struct. **114**, 64–79 (2014)
13. L. Yao, Y. Sun, M. Zhao, R.C. Alderliesten, R. Benedictus, Stress ratio dependence of fibre bridging significance in mode I fatigue delamination growth of composite laminates. Compos. Part A Appl. Sci. Manuf. **95**, 65–74 (2017)
14. P.M.V. Rao, V.V. Subba Rao, Degradation model based on Tsai–Hill factors to model the progressive failure of fiber metal laminates. J. Compos. Mater. **45**(17), 1783–1792 (2011)
15. P.M.V. Rao, V.V.S. Rao, Estimating the failure strength of fiber metal laminates by using a hybrid degradation model. J. Reinf. Plast. Compos. **29**(20), 3058–3063 (2010)
16. P. Iaccarino, A. Langella, G. Caprino, A simplified model to predict the tensile and shear stress–strain behaviour of fibreglass/

aluminium laminates. Compos. Sci. Technol. **67**(9), 1784–1793 (2007)
17. G.J. Turvey, An initial flexural failure analysis of symmetrically laminated cross-ply rectangular plates. Int. J. Solids Struct. **16**(5), 451–463 (1980)
18. E. Science, A first-ply failure analysis composite laminates. Comput. Methods Appl. Mech. Eng. **25**(3), 371–393 (1986)
19. G.S. Ramtekkar, Y.M. Desai, A.H. Shah, First ply failure of laminated composite plates-a mixed finite element approach. J. Reinf. Plast. Compos. **23**(3), 291–315 (2004)
20. C. Ray, S.K. Satsangi, Laminated stiffened plate—a first ply failure analysis. J. Reinf. Plast. Compos. **18**(12), 1061–1076 (1999)
21. C.F. Lü, W.Q. Chen, J.W. Shao, Semi-analytical three-dimensional elasticity solutions for generally laminated composite plates. Eur. J. Mech. A. Solids **271**(5), 899–917 (2008)
22. M.W. Hyer, *Stress Analysis of Fiber-Reinforced Composite Materials* (TMH, Mumbai, 1998)
23. J.N. Reddy, *Theory and Analysis of Elastic Plates and Shells* (Taylor & Francis Group, Milton Park, 2007)
24. M. Kawai, M. Morishita, S. Tomura, K. Takumida, Inelastic behavior and strength of fiber-metal hybrid composite: Glare. Int. J. Mech. Sci. **40**(2–3), 183–198 (1998)
25. A.S. Kaddour, M.J. Hinton, P.D. Soden, A comparison of the predictive capabilities of current failure theories for composite laminates: additional contributions. Compos. Sci. Technol. **64**(3–4), 449–476 (2004)
26. S. Lyu, Y. Sun, G. Li, W. Xiao, C. Ma, Effect of layer sequence on the mechanical properties of Ti/TiAl laminates. Mater. Des. **143**, 160–168 (2018)
27. A.P. Sharma, S.H. Khan, R. Kitey, V. Parameswaran, Effect of through thickness metal layer distribution on the low velocity impact response of fiber metal laminates. Polym. Test. **65**(October 2017), 301–312 (2018)
28. G.H. Majzoobi, H. Morshedi, K. Farhadi, Thin-walled structures the effect of aluminum and titanium sequence on ballistic limit of bi–metal. Thin Walled Struct. **122**(October 2017), 1–7 (2018)